

COMPLEX DUNES IN THE SOUTHERN HEMISPHERE OF MARS: AGE AND WIND REGIMES. S. Silvestro¹, L. K. Fenton² and G. G. Ori^{1,3}, ¹International Research School of Planetary Sciences, Università d'Annunzio, Pescara, Italy (simone@irsps.unich.it), ²Carl Sagan Center, Mountain View, CA, USA, ³Ibn Battuta Centre, Faculté de Seances Semlalia Université Cadi Ayyad, Marrakech, Morocco

Introduction: Compound and complex dunes (draas defined by Wilson [1]) are present in most of the sand seas of the Earth [1, 2]. These bedforms are characterized by the presence of smaller dunes climbing up the stoss and the lee sides of the main one. In the case of complex dunes however, the superimposed bedforms differ in morphology from the main dune. Investigation of various images types (HRSC, THEMIS visible, MOC NA) draped on MOLA and HRSC DEMs, suggests the existence of a possible complex dune inside a crater in the eastern part of Thaumasia region (41° S ; 298° E).

Methodology: All the images of the studied area were processed using ISIS and VICAR software, and projected in a sinusoidal projection. DTMs were derived from stereo images from the HRSC camera (orbit 2431). All the datasets were integrated into a GIS project. Modeled winds were obtained from the NASA Ames Research Center general circulation model (GCM) [3, 4]. The most recent version of the Ames GCM includes an updated radiation code, a water cycle simulation, and dust prescribed by Thermal Emission Spectrometer (TES) dust opacities. The output discussed is from the nearest grid point in a 5° x 6° simulation, representing regional but not local flows.

Observation: The complex dune is shown in Fig. 1 and Fig. 2, which appear to show a large bedform with superimposed smaller dunes. The complex dune is 400 m high and 11 km wide and is located in a crater of 53 km in diameter. The morphology of the superimposed dunes is complicated. The north-eastern side of the main dune is covered by barchans dunes, whereas the south-western slope and near the crest star and reversing dunes are present. On the north-western part of the crater, barchans show two different slip face orientations (Fig. 2a). This morphology is not observed on Earth, but it may be common on Mars [5, 6]. The wind directions derived from the slip face orientations indicate a convergence of different winds that could explain the pile-up of the dunes in a single, high, complex bedform. The profiles (Figs. 3a, 3b) obtained from MOLA and HRSC DTMs, show that the north-eastern slope of the main dune is steeper than the other side. Although the slope angle is too low (7°– 17°) to be considered an avalanching slip-face, this value could be at least considered an index of the overall bedform migration towards the northeastern rim of the

crater. In the Fig 4a the plot of the GCM output represents the direction and magnitude of the wind stresses in degrees clockwise from north (0° = winds from the north, 90° = winds from the east, etc).

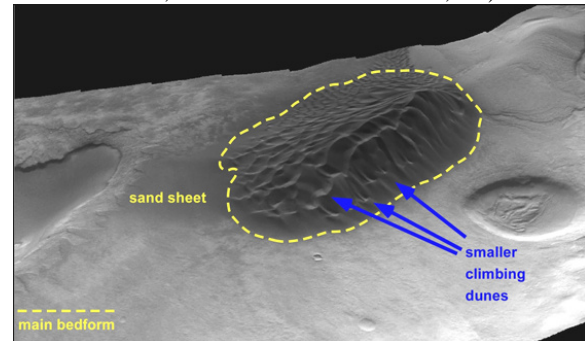


Fig.1, main dune with smaller barchans superimposed on the NE slope (lee side). THEMIS Vis V09939001 draped on HRSC DTM (vertical ex. x 4).

The first plot shows winds stronger than 0.005 N m⁻² (this cutoff value was chosen not as a saltation threshold but rather as an arbitrary limit to indicate strong winds that may be locally enhanced to produce saltation), as function of local time and direction (the larger the box, the stronger the winds). Figs. 4b and 4c are the seasonal division of the yearly data shown in Fig. 4a. From Ls=90-180 (winter) strong winds blows from the west while from Ls=270-360 (summer) strong winds blow from the west, but also from the south and east.

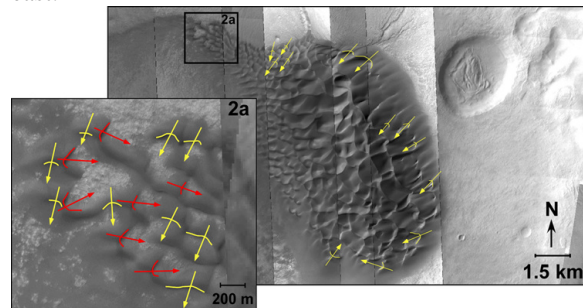


Fig.2, slip face orientations of the superimposed dunes

Discussion: From the 3D view of the bedform (Fig. 1) it is suggested that the dark erg is a complex single dune. Two winds, from west and east, are required to accumulate such a complex and high large bedform inside the crater. The GCM results show that strong winds from West (between 225° - 315°) are predicted

to blow most of the year, and are probably responsible of the overall shape and migration of the main dune towards the north-eastern part of the crater wall. Easterly winds are also predicted to blow in the summer period and are probably enhanced and influenced by the crater wall, balancing out the westerly winds and causing the sand to pile up inside the crater. Barchans in the northwestern part of the crater (Fig. 2a) have two slip face orientations (from WSW-WNW, red arrows, and from NE, yellow arrows), which may reflect the dominant modeled winds (although perhaps modified by local topography). Slip faces of the superimposed dunes on the western slope (lee side) of the main bedforms are oriented towards southwest, likely influenced by secondary winds blowing in summer. Thus the shape and position of this complex dune corresponds well with the wind regime predicted by the GCM.

Conclusions: Several clues justify the identification of this bedform as a complex dune, the main reason being the presence of smaller climbing dunes of different morphology on both sides. Furthermore, the presence of a complex wind regime is predicted by the GCM model and deduced by the slip face orientation of the superimposed dunes. The wind regime reconstructed by the GCM reflects the current atmospheric pattern and this suggest that these bedforms probably formed in present day atmospheric conditions or under atmospheric conditions similar to the present ones. The convergence of several winds from different direction is necessary to pile-up the dunes and accumulate the sediment in a high complex dune (400 meter in height measured on MOLA DTM). Another possible complex bedform is situated nearby (43.7° S ; 297.7° E). The acquisition of GCM data and further investigation of the area near Argyre could lead to a better understanding of the origin of these complex bedforms on Mars.

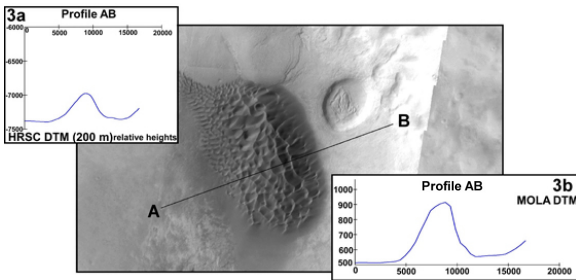


Fig.3. profile AB on HRSC (3a) and MOLA (3b) DTMs

References: [1] Wilson I. G. (1972a) *Sedimentology*, 19, 173–210. [2] McKee E. D. (1978) *USGS Professional Paper no. 1052*. [3] Haberle et al. (2006) *GRL* 33, L19S04. [4] Kahre et al. (2006) *JGR* 111(E6), E06008. [5] Fenton L. K. et al (2005)

JGR, 110, E11004. [6] Hayward R. K. et al. (2008), *this volume LPSC 39*, Abst. # .

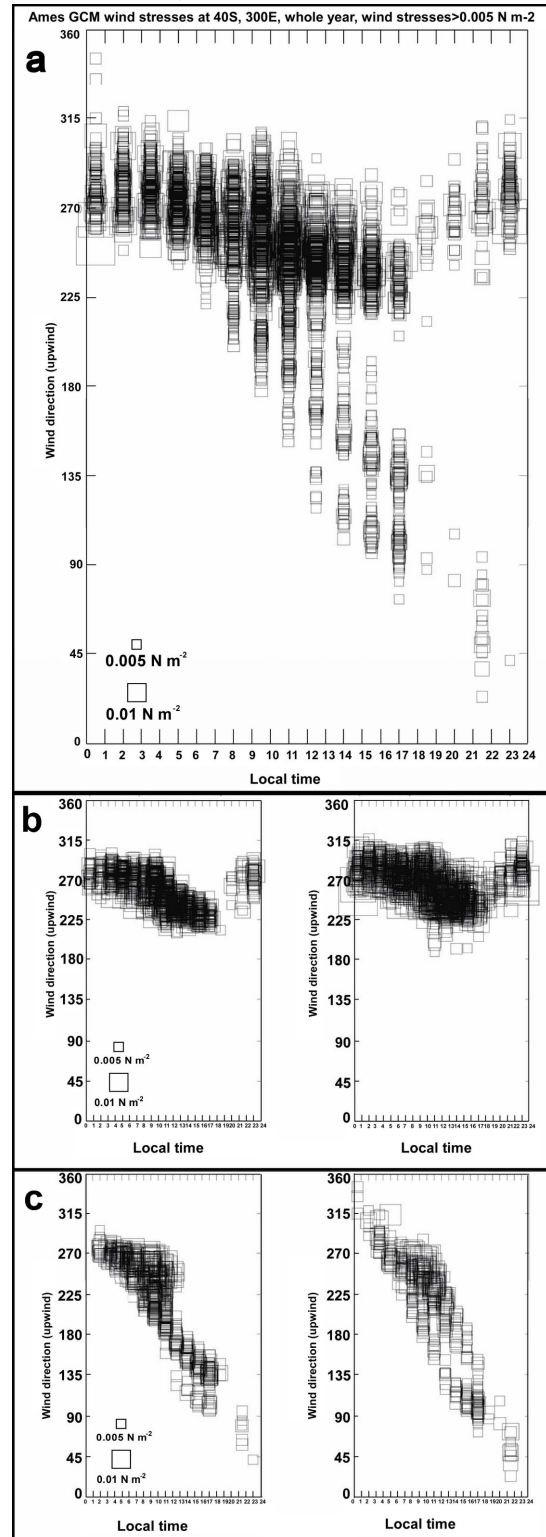


Fig.4. GCM output whole year (a), winter: $L_s=0^\circ-90^\circ$, $90^\circ-180^\circ$ (b), summer: $L_s=180^\circ-270^\circ$, $270^\circ-360^\circ$ (c)